

Synthesis and characterization of microwave irradiated Sr doped ZnO nanostructure

L. BRUNO CHANDRASEKAR^{a,*}, S. NAGARAJAN^b, P. RAMASUNDARI^c, R. VIJAYALAKSHMI^d, M. KARUNAKARAN^e, T. DANIEL THANGADURAI^f

^aDepartment of Physics, The American College, Madurai, India

^bDepartment of Chemistry, NIT-Manipur, Imphal, India

^cDepartment of Physics, NMSSVN College, Madurai, India

^dPG and Research Department of Physics, Thiagarajar College, Madurai, India

^eDepartment of Physics, Alagappa Govt. Arts College, Karaikudi, India

^fDepartment of Nanoscience and Technology, Sri Ramakrishna Engineering College, Coimbatore, India

Sr doped ZnO nanostructure was prepared by chemical precipitation method and it was irradiated by microwave. The X-ray diffraction studies show that the material has hexagonal phase in nature and the unit cell analysis were done. The unit cell properties such as nearest-neighbour bond length, second-nearest neighbour bond length and bond angles were examined and reported. Purity of the nanostructure was confirmed by the energy dispersive X-ray analysis and morphological analysis were carried out by scanning electron microscopy. Urbach energy and band gap were estimated using the optical absorption spectrum. The intensity of the photoluminescence spectrum depends on the doping concentration of Sr.

(Received April 23, 2018, accepted February 12, 2019)

Keywords: Nanostructure, Hexagonal, Urbach energy, Photoluminescence

1. Introduction

ZnO is one of the most studied materials of the II-VI semiconductors that derive continuous attention of the researchers worldwide for a very long time [1]. Due to the potential application of undoped and doped ZnO in various fields such as UV absorbers, dental cement, optical coatings, nonlinear optical switch, antimicrobial material, heaters, chemical sensors and transparent conductor [2-9], the researchers show increasing interest in estimating its properties and more devices are added these days. ZnO has a wide direct band gap of 3.37 eV at room temperature and a large excitation binding energy of about 60 meV [10]. The properties of low dimensional ZnO such as thin film, nanorod, nanoflowers, nanowire and nanostructure are reported by several groups [11-16]. Different synthesis methods are available to prepare low dimensional ZnO such as SILAR [13], microwave irradiation [10], hydrothermal method [17], sonochemical method [4], sol-gel spin coating method [18] and gas condensation process [19].

In this work, transition metal (Sr) doped ZnO nanostructure are prepared by chemical precipitation method and is characterized by X-ray diffraction (XRD), scanning electron microscope (SEM), energy dispersive X-ray analysis (EDX), optical absorption and photoluminescence (PL) technique to study its structural, morphological, chemical compositional and optical properties respectively. In this paper, the experimental procedure to prepare the Sr doped ZnO nanostructure, the results of characterization and the detailed discussions are presented in sequence.

2. Experimental procedure

Chemical precipitation is simple and cost effective method to prepare doped ZnO nanostructure. All the chemicals which are used in this process are analytical reagent grade (AR). A typical procedure for the synthesis of Sr doped ZnO nanostructure is as follows: Zn(NO₃)₂·6H₂O and nitrate salt of corresponding transition metal are weighted as per the stoichiometric ratio and dissolved in 100 ml of deionized water to make 0.2 M of solution. The solution is taken in a conical flask and the solution is constantly stirred. The NaOH solution is taken in a burette and added drop wise to get the pH value of 10. 0.2 M of EDTA is used as a capping agent in this process. The obtained precipitate is washed several times and irradiated with microwave in the microwave oven for 5 min. The samples are characterized using XRD, SEM, EDX, UV-Vis-NIR spectrometer and PL.

3. Results and discussion

3.1. X-ray diffraction

Micro-structural properties of nano materials can be easily found out using X-ray diffraction technique. Fig. 1 shows the typical XRD pattern of Sr doped ZnO nanostructure which corresponds to wurzite geometry. The XRD pattern is compared with the undoped ZnO. The (002) is the dominant peak in the observed pattern when the Sr is doped in the Zn lattice. Change in the intensity and shift of the peak in XRD due to the variation of doping

concentration of Sr in Zn lattice were observed. The grain size of the prepared nanomaterial is estimated by Debye-Scherrer's formula and it is given by

$$D = \frac{k\lambda}{\beta \cos\theta} \quad (1)$$

where k is a constant, λ is the wavelength of Cu-K α line and β is full-width at half maximum. For 5% and 10% Sr doped ZnO nanostructure, the observed grain size is 13 nm and 17 nm, respectively. This clearly indicates that low doping concentration of Sr in the Zn lattice leads to the lowering of grain size. This is in agreement with the results reported by A.Ouhaibi *et al.* [20]. This is due to the fact that the atomic radii of Sr²⁺ is higher than the Zn²⁺. Using the formula, $\delta = \frac{1}{D^2}$, the dislocation density is calculated. Let 'n' be the number of peaks and $I(hkl)$ be the intensity of peak, the texture coefficient is given by

$$TC = \frac{n \times 100}{\sum I(hkl)} \quad (2)$$

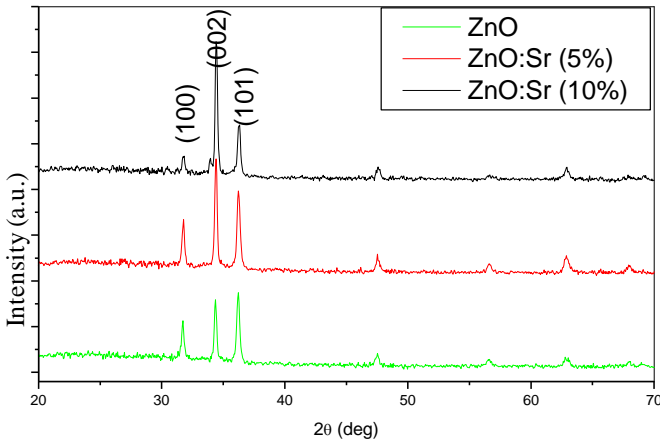


Fig. 1. XRD pattern

The texture coefficient greater than one indicates the well textured nanostructure formation. Here 5 peaks with greater intensity are considered for further calculation and hence $n = 5$. The calculated value of texture coefficient is greater than one, hence the observed material is a crystalline, not amorphous. The estimated values are presented in Table 1. To find the true lattice constant a_0 and c_0 , Nelson-Riley function (NRF) is used and is given as

$$NRF = 0.5 \left(\frac{\cos^2 \theta}{\sin \theta} + \frac{\cos^2 \theta}{\theta} \right) \quad (3)$$

Table 1. Micro-structural properties

	ZnO:Sr (5%)	ZnO:Sr (10%)
Grain size	13 nm	17 nm
Dislocation density	$5.9 \times 10^{15}/m^2$	$3.5 \times 10^{15}/m^2$
Texture coefficient	1.4	1.6

The calculated NRF is taken along the horizontal axis and the lattice constant which is calculated from

$$d^{-2} = \frac{4}{3} \left(\frac{h^2 + hk + k^2}{a^2} \right) + \frac{l^2}{c^2} \quad (4)$$

(where h , k and l indicate the miller indices) are taken along the vertical axis. The extrapolation of the linear fit to vertical axis gives the value of true lattice constant. Fig. 2 and 3 show the variation of NRF vs. lattice constant for 5% and 10% Sr doped ZnO nanostructure, respectively. The unit cell representation of ZnO is shown in Fig. 4. The

nearest neighbour bond length $b_1 = \sqrt{\frac{a_0^2}{3} + \left(\frac{1}{4} - \frac{a_0^2}{3c_0^2}\right)^2 c_0^2}$,

three types of second-nearest neighbour distances $b'_1 = c_0(1 - u)$, $b'_2 = \sqrt{a_0^2 + (uc)^2}$ and

$b'_3 = \sqrt{\frac{4}{3}a_0^2 + c_0^2\left(\frac{1}{2} - u\right)^2}$ are calculated [21]. The

calculated value of true lattice constant, nearest neighbour distances and bond angles are given in Table 2. The observed values agree well with standard results. The lattice constant, bond length and the nearest neighbour distances are depends on the doping concentration of Sr.

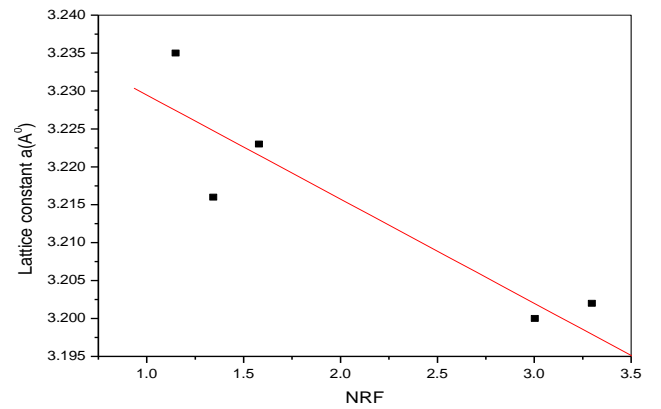
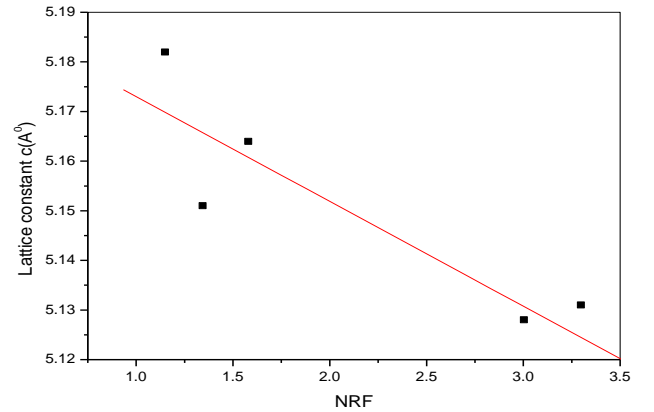


Fig. 2. Lattice constant vs. NRF for ZnO:Sr (5%)

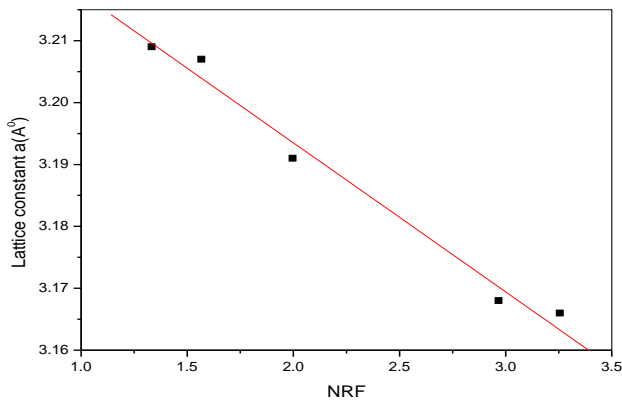
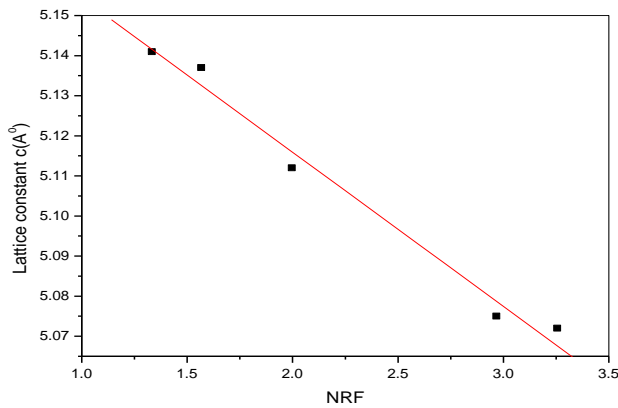


Fig. 3. Lattice constant vs. NRF for ZnO:Sr (10%)

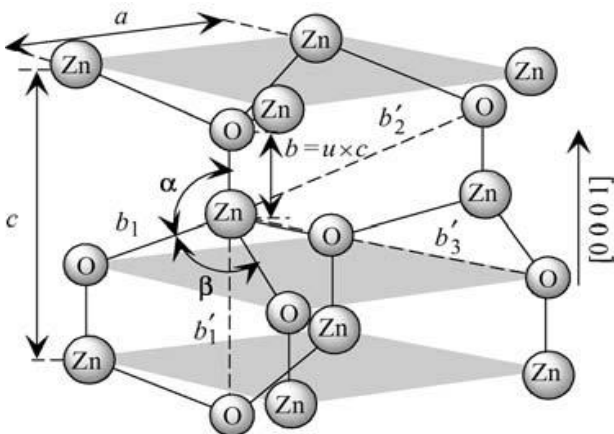


Fig. 4. Unit cell representation of ZnO

Table 2. Unit cell properties

Unit cell parameters	ZnO:Sr (5%)	ZnO:Sr (10%)
Lattice constant a_0	3.238 Å	3.251 Å
Lattice constant c_0	5.185 Å	5.192 Å
Bond length	1.971 Å	1.976 Å
Second-nearest neighbour distance b'_1	3.209 Å	3.214 Å
Second-nearest neighbour distance b'_2	3.792 Å	3.804 Å
Second-nearest neighbour distance b'_3	3.792 Å	3.804 Å

3.2. Surface morphology and compositional studies

Fig. 5 shows the SEM micrograph obtained for the prepared samples with magnification of 20,000. The formed nanostructure is clearly shown in the image. The nano-plate structure is observed and the change in the dimension of the nano-plate is due to the change in concentration of Sr. Fig. 6 shows the EDX spectrum of the prepared samples. It clearly indicates that the samples consist Zn, O and Sr. No impurities are found which means the phase purity of Sr doped ZnO and the superiority of the chemical precipitation method.

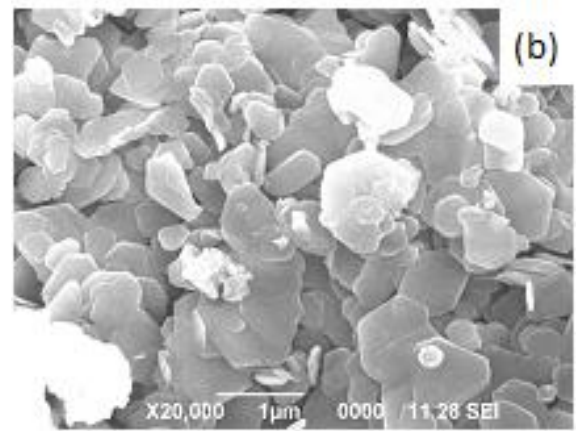
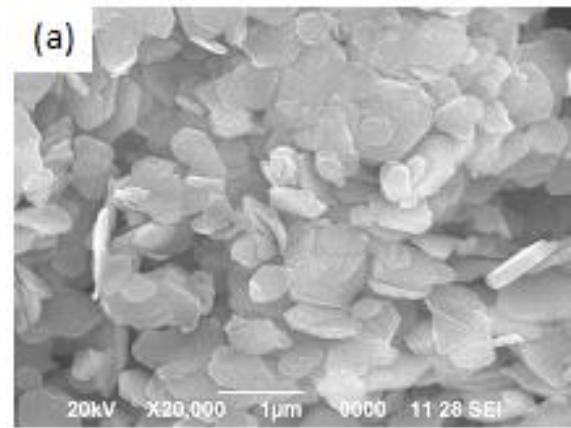


Fig. 5. SEM photograph: (a) ZnO:Sr (5%) and (b) ZnO:Sr (10%)

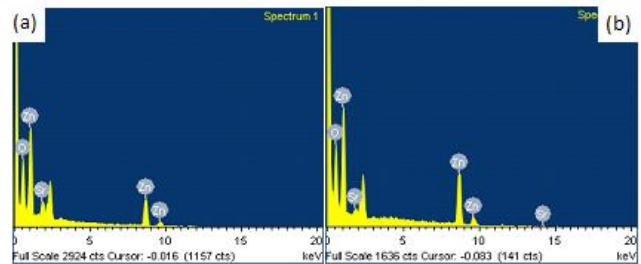


Fig. 6. EDX Spectrum

3.3. Optical properties

The simple and direct method for probing band structure is the optical absorption spectrum. The absorption as a function of wavelength is shown in Fig. 7. The linear portion in the figure indicates the direct type transition. The prepared samples have the maximum absorption which is blue shifted as compared with the bulk ZnO due to the quantum confinement. The absorption edge is analysed using the expression

$$\alpha hv = A(hv - E_g)^n \quad (5)$$

where 'm' is chosen as 0.5 or 2, according to either the material is direct band gap or indirect band gap material and α is the absorption coefficient. The variation of αhv^2 vs. hv is shown in Fig. 8. The intercepts of the straight line portion to the horizontal axis give the band gap of the material. The observed value of band gap for 5% and 10% Sr doped ZnO is, respectively, 3.85 eV and 4.07 eV. The increasing doping concentration enhances the band gap in the case of Sr doped ZnO. This is in line with the reported result [20]. The variation of $\ln(\alpha)$ vs. hv is shown in Fig. 9. The reciprocal gradient of the straight line fit in the variation of $\ln(\alpha)$ is the Urbach energy and the observed values are 320 meV and 313 meV, respectively, for 5% and 10% Sr doped ZnO nanostructure. The photoluminescence spectrum of prepared samples at room temperature is shown in Fig. 10. The peak near 330 nm corresponds to near band edge emission of the wide band gap of Sr doped ZnO. As the doping concentration of Sr increases, the photoluminescence intensity of the sample decreases and is due to the effect of quenching. The intensity of the peak around 475 nm (which is due to the recombination electron-hole pair) decreases due to the high concentration of Sr, This implies that the Sr addition in Zn lattice reduces the photocatalytic activity due to the lower recombination rate. The defect concentration is also responsible for this observation. The observed results indicate the suitability of fabricating ZnO nanostructures based devices. Especially Sr doped ZnO has high absorption in the UV region, the ideas and the observed results can be useful for fabrication UV absorbers.

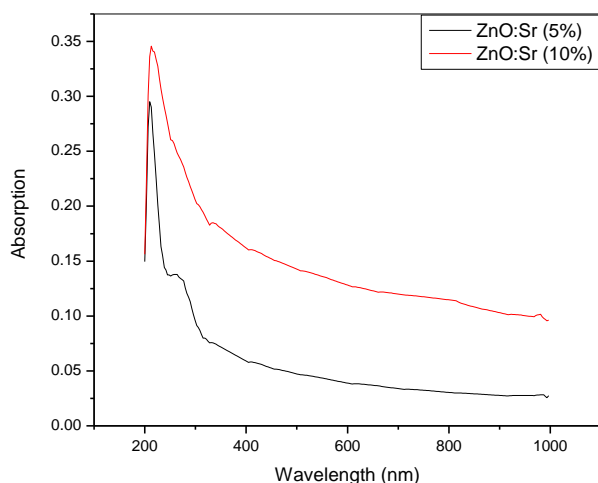


Fig. 7. Absorption spectrum

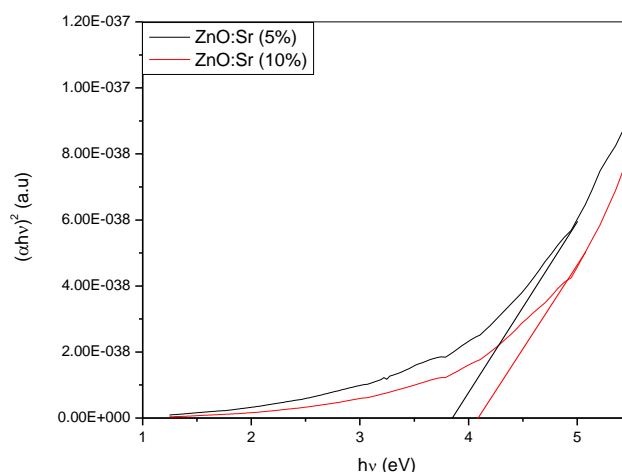


Fig. 8. Tauc's plot

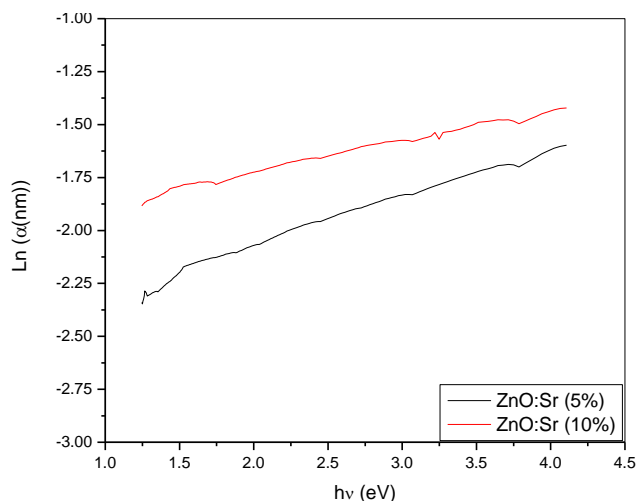


Fig. 9. $\ln(\alpha)$ vs. hv

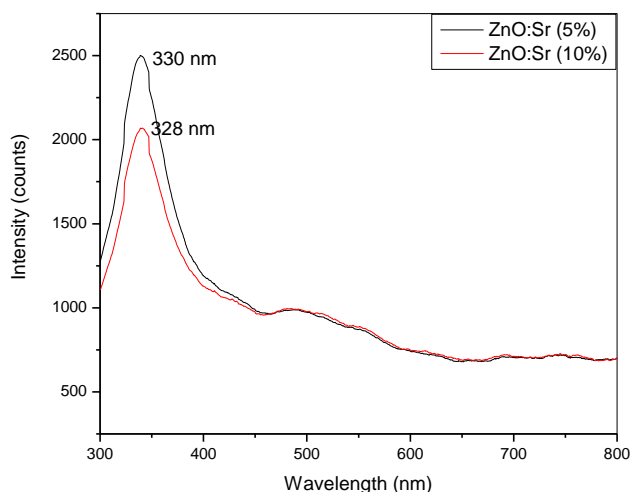


Fig. 10. Photoluminescence spectrum

4. Conclusion

Microwave irradiated Sr doped ZnO nanostructure are prepared and characterized. Micro-structural properties and unit cell information are calculated from the XRD data. The EDX shows that the samples are high pure in nature. The wide band gap upto 4.07 eV is observed in Tauc's plot and Urbach energy is also calculated. The near band gap emission is observed in Photoluminescence spectrum. The doping of Sr influences the micro-structural and optical properties of ZnO. This work aims to induce further experimental work on Sr doped ZnO nanostructure.

References

- [1] C. W. Bunn, Proc. Phys. Soc. London **47**, 835 (1935).
- [2] Alessio Becheri, Maximilian Durr, Pierandrea Lo Nostro, Piero Baglioni, J. Nanopart. Res. **10**, 679 (2008).
- [3] R. Rajendran, C. Balakumar, Hasabo A. Mohammed Ahammed, S. Jayakumar, K. Vaideki, E. M. Rajesh, Int. J. Eng. Sci. & Tech. **2**, 202 (2010).
- [4] Mohammad Ali Karimi, Saeed Haghdar Roozbahani, Reza Asadiniya, Abdolhamid Haatefi-Mehrjardi, Mohammad Hossein Mashhadizadeh, Reza Behjatmanesh-Ardakani, Mohammad Mazloun-Ardakani, Hadi Kargar, Seyed Mojtaba Zebarjad, Int. Nano Lett. **1**, 43 (2011).
- [5] Yanwu Zhu, Hendry Izaac Elim, Yong-Lim Foo, Ting Yu, Yanjiao Liu, Wei Ji, Jim-Yang Lee, Zexiang Shen, Andrew Thye-Shen Wee, John Thiam-Leong Thong, Chong-Haur Sow, Adv. Mater. **18**, 587 (2006).
- [6] S. H. Jeong, B. N. Park, D. G. Yoo, J. H. Boo, J. Korean Phys. Soc. **50**, 622 (2007).
- [7] S. Mondal, K. P. Kanta, P. Mitra, J. Phys. Sci. **12**, 221 (2008).
- [8] Alessio Becheri, Maximilian Durr, Pierandrea Lo Nostro, Piero Baglioni, J. Nanopart. Res. **10**, 679 (2008).
- [9] Chin-Cheng Hsu, N. L. Wu, Journal of Photochemistry and Photobiology A: Chemistry **172**, 269 (2005).
- [10] Seungho Cho, Seung-Ho Jung, Kun-Hong Lee, J. Phys. Chem. C **112**, 12769 (2008).
- [11] Sheo K. Mishra, Rajneesh K. Srivastava, S. G. Prakash, J. Mater. Sci.: Mater. Electron. **24**, 125 (2013).
- [12] N. Faal Hamedani, F. Farzaneh, J. Sci. **17**, 231 (2006).
- [13] A. Raidou, M. Aggour, A. Qachaou, L. Laanab, M. Fahoume, J. Condens. Matter **12**, 125 (2010).
- [14] Po-Yi Wu, Jenna Pike, Feng Zhang, Siu-Wai Chan, Int. J. Appl. Ceram. Technol. **3**, 272 (2006).
- [15] J. Carrey, M. L. Kahn, S. Sanchez, B. Chaudret, M. Respaud, Eur. Phys. J. Appl. Phys. **40**, 71 (2007).
- [16] Rizwan Wahab, S. G. Ansari, Y. S. Kim, H. K. Seo, G. S. Kim, Gilson Khang, Hyung-Shik Shin, Mat. Tes. Bull. **42**, 1640 (2007).
- [17] D. Sridevi, K. V. Rajendran, Int. J. Nanotech. Appl. **3**, 43 (2009).
- [18] S. Ilican, Y. Caglar, M. Caglar, J. Optoelectron. Adv. M. **10**(10), 2578 (2008).
- [19] Ho Chang, Ming-Hsun Tsai, Rev. Adv. Mater. Sci. **18**, 734 (2008).
- [20] A. Ouhaibi, M. Ghamnia, M. A. Dahamni, V. Heresanu, C. Fauquet, D. Tonneau, J. Sci: Adv. Mat. Devices **3**, 29 (2018).
- [21] L. Bruno Chandrasekar, R. Chandramohan, S. Chandrasekaran, J. Thirumalai, R. Vijayalakshmi, Adv. Sci. Focus **1**, 292 (2013).

*Corresponding author: brunochandrasekar@gmail.com